Assessment of the effects of amphiphilic poly (N-vinylpyrrolidone) nanoparticles loaded with bortezomib on glioblastoma cell lines and zebrafish embryos

ANNE V. YAGOLOVICH[1*], ANDREY N. KUSKOV[2*], PAVEL P. KULIKOV[2], DMITRY V. BAGROV[1], POLINA A. PETROVA[1], EKATERINA V. KUKOVYAKINA[2], ALINA A. ISAKOVA[2,3], IRINA I. KHAN[4,5], VADIM S. POKROVSKY[4,5], ALEXANDER E. NOSYREV[6], POLYXENI C. STAMATI[7], ELENA A. MARKVICHEVA[3], MARINE E. GASPARIAN[2,3], DEMETRIOS A. SPANDIDOS[8] and ARISTIDIS M. TSATSAKIS[6,9]

[1]Faculty of Biology, Lomonosov Moscow State University, 119234 Moscow; [2]D. Mendeleev University of Chemical Technology of Russia, 125047 Moscow; [3]Shemyakin-Ovchinnikov Institute of Bioorganic Chemistry of The Russian Academy of Sciences, 117997 Moscow; [4]N.N. Blokhin National Medical Research Center of Oncology, Ministry of Health of Russia, 115478 Moscow; [5]Medical Institute, Patrice Lumumba People's Friendship University, 117198 Moscow; [6]Center of Bioanalytical Research and Molecular Design, Sechenov First Moscow State Medical University, 119991 Moscow, Russian Federation; [7]Department of Neurology, University Hospital of Larissa, Faculty of Medicine, School of Health Sciences, University of Thessaly, 41100 Larissa; [8]Laboratory of Clinical Virology, Faculty of Medicine; [9]Center of Toxicology Science and Research, Division of Morphology, Medical School, University of Crete, 71003 Heraklion, Greece

Received October 25, 2023; Accepted January 4, 2024

DOI: 10.3892/br.2024.1725

Abstract. Proteasome inhibitor bortezomib is an anticancer agent approved for treatment of multiple myeloma and mantle cell lymphoma. However, its application in other types of cancer, primarily in solid tumors, is limited due to poor pharmacokinetics, inefficient tissue penetration, low stability and frequent adverse effects. In the present study, a novel micellar nano-scaled delivery system was manufactured, composed of amphiphilic poly(N-vinylpyrrolidone) nanoparticles loaded with bortezomib. Similar nanoparticles loaded with prothionamide, a drug without anticancer effect, were used as control. The size and zeta potential of the obtained polymeric micelles were measured by dynamic light scattering. Bortezomib-loaded micelles exhibited significant cytotoxic activity *in vitro* in monolayer tumor cell cultures (IC_{50} ~6.5 μg/ml) and in 3D multicellular tumor spheroids (IC_{50} ~8.5 μg/ml) of human glioblastoma cell lines U87 and T98G. Additionally, the toxic effects *in vivo* were studied in zebrafish *Danio rerio* embryos, with an estimated 50% lethal concentration of 0.1 mg/ml. Considering that bortezomib and other molecules from the class of proteasome inhibitors are potent antitumor agents, nanodelivery approach can help reduce adverse effects and expand the range of its applications for treatment of various oncological diseases.

Correspondence to: Professor Andrey N. Kuskov, D. Mendeleev University of Chemical Technology of Russia, Miusskaya Square 9, Building 6, 125047 Moscow, Russian Federation
E-mail: kuskov.a.n@muctr.ru

Dr Anne V. Yagolovich, Faculty of Biology, Lomonosov Moscow State University, 1/12 Leninskie Gory, 119234 Moscow, Russian Federation
E-mail: anneyagolovich@gmail.com

*Contributed equally

Key words: amphiphilic, poly(N-vinylpyrrolidone), polymer nanop-articles, micelles, bortezomib

Introduction

The prominent antitumor potential of proteasome inhibitors was discovered in 1999 and immediately attracted attention of scientists and medical oncologists (1). The first-in-class proteasome inhibitor bortezomib (Velcade®) became one of the most rapidly developed antitumor agents in recent history with 8 years from initial synthesis in 1995 to US Food and Drug Administration approval in 2003 for treatment of multiple myeloma (2). Further in 2006, bortezomib was approved for treatment of mantle cell lymphoma (3). Nevertheless, a set of limitations narrow the broadening of bortezomib's wide use beyond the treatment hematological malignancies. Similar to conventional chemotherapeutic drugs, proteasomal inhibitors including bortezomib exhibit the pronounced dose-limiting toxicities, such as thrombocytopenia and peripheral neuropathy (4,5). Bortezomib non-specifically binds to plasma proteins unselectively and is extensively metabolized by hepatic cytochrome P450 family enzymes, which attenuates its tissue penetration (6,7). Low bioavailability, partly explained by poor solubility in aqueous

solutions due to high hydrophobic properties, together with high toxicity to normal tissues limit its application in therapeutic regimens for the treatment of solid tumors.

Polymers are extensively studied as perspective systems for drug delivery due to their tunable properties, optimal pharmacokinetics, biodegradability and safety. Polymer nanocarriers with immobilized drugs show off increased efficiency due to their favorable delivery, ability of administration with poorly soluble active substances, increased biocompatibility and bioavailability, low effective doses, controlled release and prolonged effect of the drugs from the polymeric system (8). Therefore, nanodelivery approach can contribute to the improvement of bortezomib tissue distribution and reduction of its adverse effects. In this regard, polymer poly(N-vinylpyrrolidone) (PVP) has unique properties, extensively reviewed in the literature (9), which make it suitable for nanodelivery applications and namely flexible design. It has favorable solubility in both inorganic and organic solvents, ability to carry both hydrophilic and hydrophobic substances, lack of toxicity, and it is eco-friendly.

Previously, it has been demonstrated by the authors that polymeric micelles composed of amphiphilic PVP are suitable for the delivery of a wide variety of therapeutic molecules encapsulated in their core, with high hydrophobicity as a main requirement. For example, PVP micelles recently acted as nanocarriers for the anti-inflammatory non-steroidal drug indomethacin (10), demonstrated stability in blood serum and excellent blood compatibility, quaintly without initiating the complement cascade or decreasing the potential of the system (11,12). On the contrary, they appeared to protect the endothelium (13).

A technique for production of PVP-based micelles loaded with prothionamide, an anti-tuberculosis drug without anticancer effect, has been previously described. It was used as a highly hydrophobic core for micelles bearing antitumor receptor-specific protein based on human cytokine TRAIL on their surface (14). In the present study, the use of a similar technology for encapsulation of the proteasome inhibitor bortezomib into micellar nanoparticles composed of amphiphilic PVP was pioneered. The production and characterization of the bortezomib-loaded micellar nanoparticles, investigation of toxicity *in vitro* in human 2D and 3D models of human glioblastoma, and *in vivo* in zebrafish embryos, was further reported. The newly obtained PVP-B micelles can become a perspective nanoplatform for improved delivery of bortezomib, broadening the range of its applications to the treatment of solid tumors.

Materials and methods

Materials and reagents. AIBN (2,2'-azobisisobutyronitrile), 1,4-dioxane and VP (N-vinyl-2-pyrrolidone) were obtained from Acros (https://www.thermofisher.com/ru/en/home/chemicals/acros-organics.html). Stearoyl chloride, DMSO (dimethylsulfoxide), potassium tert-butylate, prothionamide and MTT reagent (3-(4,5-dimethylthiazol-2-yl)-2,5-diphenyl-2H-tetrazolium bromide) were purchased from Sigma-Aldrich; Merck KGaA. Bortezomib was obtained from Santa Cruz Biotechnology, Inc. Dulbecco's Modified Eagle Medium (DMEM), trypsin-versene solution and PBS were purchased from PanEco. Fetal bovine serum (FBS) was purchased from HyClone; Cytiva. Cyclo-RGDfK(TPP) peptide was a kind gift of Professor S. Burov (Cytomed JSC, St-Petersburg, Russia).

Production of the micelles. The amphiphilic micellar nanoparticles were produced as previously described (14). Briefly, amphiphilic poly-N-vinylpyrrolidone with number-average molecular weight of 6 kDa and one end stearoyl hydrophobic group was synthesized via radical monomer polymerization in dioxane. Stearoyl chloride was used both as a regulator of the chain growth and a chain-transfer agent. Further, polymerization reaction between VP monomer, stearoyl chloride and initiator (dissolved in dioxane) was held for 2 h at 80˚C. The synthesized polymer was dissolved in 5 volumes of double deionized water, dialyzed in a molecular weight cut-off of 12 kDa Dialysis Cassette Slide-A-Lyzer (Thermo Fisher Scientific, Inc.) against double deionized water for 72 h, and freeze-dried using Martin Christ GmbH device. The titration analysis and vapor pressure osmometry using Knauer device and polystyrene standards in toluene solution were applied for determination of PVP number-average molecular weight.

Emulsification was applied to manufacture the micelles with incorporated prothionamide or bortezomib. Polymer suspension in water was mixed with prothionamide or bortezomib solution in chloroform and homogenized by ultrasound for 12 min under supercooling. Further, chloroform was evaporated using Heidolph Hei-VAP Value Digital device. Non-encapsulated drug was deleted by centrifugation at for 5 min at 4,000 x g using Sigma 4-5L centrifuge.

Drug loading characteristics of amphiphilic PVP nanoparticles. The content of bortezomib or prothionamide in drug-loaded polymeric nanoparticles and efficiency of encapsulation process were evaluated by determining of non-encapsulated drug quantity left in supernatant after drug-loaded nanoparticles preparation and centrifugation.

The drug loading capacity (DLC) and drug loading efficiency (DLE) of the amphiphilic PVP nanoparticles was determined using a spectrophotometer (Unico 2802 UV-vis). It was confirmed that residual amounts of water in the system did not affect this calibration (15). The absorbance wavelength for bortezomib evaluation was 269 nm, and for prothionamide estimation absorbance wavelength was 294 nm. DLC of the obtained preparations was determined using following equation:

$$\text{DLC (\%)} = \frac{\text{total weight of drug used} - \text{weight of non-entrapped drug}}{\text{total weight of drug-loaded nanoparticles}} \times 100\%$$

DLE was estimated using following equation:

$$\text{DLE (\%)} = \frac{\text{total weight of drug} - \text{weight of non-entrapped drug}}{\text{total weight of drug used}} \times 100\%$$

Dynamic light scattering (DLS) and zeta potential measurements. The DLS and zeta potential measurements were carried out using a Malvern Zetasizer Nano ZS (Malvern Panalytical Ltd.). The NPs were placed into 70 μl cuvettes (BRAND GmbH) or Malvern 1070 folded capillary cells (Malvern Panalytical Ltd.) for the determination of size and zeta potential, respectively. The measurement duration was determined automatically for each run. The temperature was set to 25˚C.

To assess the influence of ultrasonic treatment on the size of the NPs, the suspensions were treated using a 60W KDL-1.3L ultrasound cleaner for 15 min on ice.

Transmission electron microscopy (TEM). TEM measurements were carried out using a JEM-1400 (JEOL, Ltd.) microscope operating at 120 kV. The formvar/carbon TEM grids were treated by a glow-discharge device Emitech K100X at 25 mA for 30 sec. The samples were deposited on the grid surface without fixative for 1 min, then the grids were blotted and stained by 1% uranyl acetate.

PVP-B cytotoxicity in vitro. Human glioblastoma cell line T98G (cat. no. CRL-1690), glioblastoma of unknown origin U87 (cat. no. HTB-14) and normal human dermal fibroblasts (cat. no. PCS-201-012) were obtained from the American Type Culture Collection. All cells were tested negative for mycoplasma contamination. Cells were cultivated in DMEM cell culture medium containing 10% FBS at 37˚C and 5% CO_2. Detachment was held by trypsin-versene solution. To create a 3D *in vitro* model, cells were seeded in 96-well plates (5,000 cells/well), and after the cells were attached to the bottom, 40 μM cyclo-RGDfK(TPP) peptide in DMEM with 10% FBS was added, as previously described (16). The multicellular tumor spheroids were formed after 72 h.

Cytotoxic activity of the developed formulations was examined using MTT test. The monolayer cells or tumor spheroids were treated with tested substances for indicated time periods. Further, 0.05% (w/v) MTT reagentwas added to each well and incubated for 4 h at 37˚C. The formed formazan crystals were resuspended in DMSO and absorbance at 570 nm was detected using iMark Microplate Reader (Bio-Rad Laboratories, Inc.). The viability was expressed in % of control using the formula: (OD of sample-OD of background)/(OD of control-OD of background) x100%.

PVP-B toxicity in vivo in zebrafish. Adult wild-type zebrafish Danio rerio AB were maintained in aquariums with an aeration and recirculation system at 28˚C, pH 6.5-7.5, with 14-h light/10-h dark photoperiod. The fish were fed twice a day according to conventional recommendations by zebrafish feed. For spawning, sexually mature 3-months old zebrafish were used. Embryos were collected and placed in zebrafish E3 embryo water (5 mM NaCl, 0.33 mM $MgSO_4$ x $7H_2O$, 0.33 mM $CaCl_2$, 0.17 mM KCl, 0.1% methylene blue).

Unfertilized eggs and embryos 24 h after fertilization that had significant developmental defects were detected under a Nexcope NSZ-810 light microscope and removed from the experiment. Experimental embryos were mechanically dechorionized with tweezers and placed in 24-well culture plates (2 embryos per well, total 1 ml of solution per well). The bortezomib-loaded PVP-B nanoparticles were added in a concentration range of 0.03-30 mg/ml in each well. Each well was performed in triplicate (n=6 per group). The embryos were examined 24 [48 h post-fertilization; (hpf)] and 72 (96 hpf) h after the addition of PVP-B; developmental disorders and delays, morphological changes, including irregular shape of the yolk sacs, impaired tail development and decreased motor activity were recorded. To estimate the range of mortality from 0 to 100%, embryonic deaths were recorded at 24 (48 hpf) and 72 (96 hpf) h after addition of PVP-B. Lethal concentration 50% (LC_{50}) was calculated at the end of the experiment from cumulative mortality by regression analysis using Graphpad Prism version 8.01 software (Dotmatics).

Zebrafish embryos were euthanized at the age of 120 hpf using a bleach solution of 1 part sodium hypochlorite 6.15% to 5 parts water according to the Guidelines for Use of Zebrafish in the NIH Intramural Research Program accepted in 2009 (https://oacu.oir.nih.gov/system/files/media/file/2023-08/b17_zebrafish.pdf), in accordance with the AVMA Guidelines on Euthanasia: 2020 Edition.

Statistical analysis. The obtained data represented normal distribution and were displayed as the mean ± SD. The experiments were held in three replicates no less than three times. In cell experiments, statistical differences were analyzed by unpaired Student's t-test. $P<0.05$ was considered to indicate a statistically significant difference. LC_{50} was determined by non-linear regression analysis in Graphpad Prism version 8.01 (Dotmatics).

Results

Production and characterization of bortezomib-loaded nanoparticles. The amphiphilic polymers composed of PVP with molecular weight of 11 kDa were synthesized by earlier developed original one-step method with 80-90% yield (17,18). The core of the self-assembled micelles was loaded with proteasomal inhibitor bortezomib by the emulsion method, which involved ultrasonic treatment of polymer solution in water jointly with bortezomib solution in chloroform. Thus, micellar PVP-B nanoparticles encapsulating bortezomib were manufactured. To compare the properties of micelles depending on loaded substances, in addition to PVP-B, the previously characterized particles PVP-P were loaded with a model substance prothionamide in similar conditions (14). The prothionamide, an antituberculosis drug (19), was chosen due to its high hydrophobicity for stabilization of the hydrophobic core of the PVP-micelles. PVP-P nanoparticles served as a model object to correctly distinguish the effect of bortezomib in PVP-B, since hollow PVP micelles that are not stabilized by a hydrophobic core may have different characteristics.

The encapsulation efficiency was 12.36 mg/g PVP for bortezomib, and 97.47 mg/g PVP for prothionamide. As the initial content of bortezomib and prothionamide in regard to PVP polymer was relatively low (~1 and 10% mass, respectively), it was possible to prepare final drug-loaded nanoparticles with DLE close to 100%, which was important in terms of rational usage of rather expensive biologically active substances, and more accurate evaluation of drug content in final nanoparticles preparations.

According to DLS, the typical size of the PVP-B nanoparticles was similar to the size of the control PVP-P nanoparticles. The peak position on the intensity distributions was 570 and 590 nm, respectively (Fig. 1A). Upon the ultrasound treatment, the peak position shifted down to 290-330 nm (Fig. 1A), and then it did not change for at least 2 days of storage at 4˚C. No precipitation was observed after ultrasound treatment.

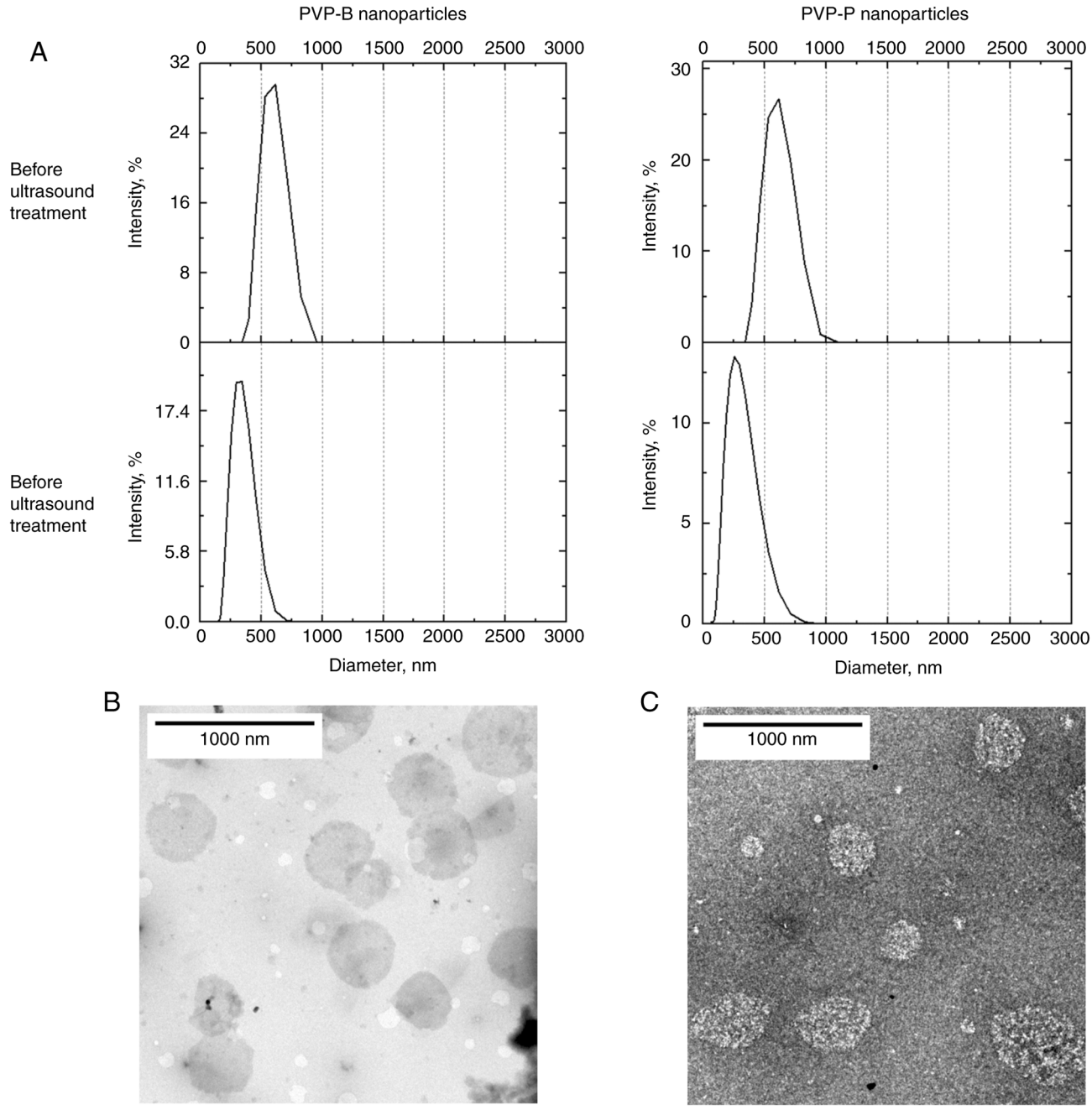

Figure 1. Characterization of the nanoparticles. (A) Measurements of the nanoparticles loaded with bortezomib and prothionamide using dynamic light scattering. The data revealed the intensity distributions before and after ultrasound treatment. (B and C) Transmission electron microscopy images of the PVP-B and PVP-P particles, respectively. PVP, poly(N-vinylpyrrolidone).

Consequently, all the substance remained encapsulated within the particles, indicating that the DLC of both PVP-B and PVP-P has not changed. The similarity of the two studied types of NPs indicated that in the current case the NP size is determined by the polymer rather than by the drug incorporated in it. When TEM was used to visualize the NPs, they appeared as roughly spherical objects with submicron size (Fig. 1B and C). All main properties of drug-loaded nanoparticles, including Z-average hydrodynamic diameter, DLC, DLE and ζ-potential, are presented in Table I.

In vitro cytotoxicity evaluation of nanoparticles. The cytotoxicity of the obtained micelles was evaluated *in vitro* in monolayer cell culture (2D) and multicellular spheroids (3D) of human glioblastoma cell lines U87 and T98G. PVP-B exhibited significant time- and concentration-dependent cytotoxicity, reaching the maximal effect after 72-h incubation. In monolayer T98G cells, IC_{50} was 6.4±1.6 μg/ml (amounting to 204.8±5.1 nM of bortezomib contents). In monolayer U87 cells, IC_{50} was 6.5±0.8 μg/ml (208.0±2.6 nM bortezomib) (Fig. 2).

As far as prothionamide was not reported to obtain antitumor activity, therefore prothionamide-loaded PVP-P micelles were used as control for PVP-B. In the present experiments, PVP-P did not obtain significant cytotoxicity in both glioma cell lines (Figs. 2 and 3). To ensure the reliability of the results, the cytotoxicity of individual substances (PVP,

Table I. Main properties of the drug-loaded amphiphilic PVP NPs.

Drug-loaded amphiphilic PVP NPs	Z-average hydrodynamic diameter, nm	Drug loading capacity, % mass	Drug loading efficiency, % mass	ζ-potential, mV
PVP-B	570	1,2	99,8	-7.7±0.4
PVP-P	590	9,8	98,3	-12.7±0.6

PVP, poly(N-vinylpyrrolidone) polymer; NPs, nanoparticles.

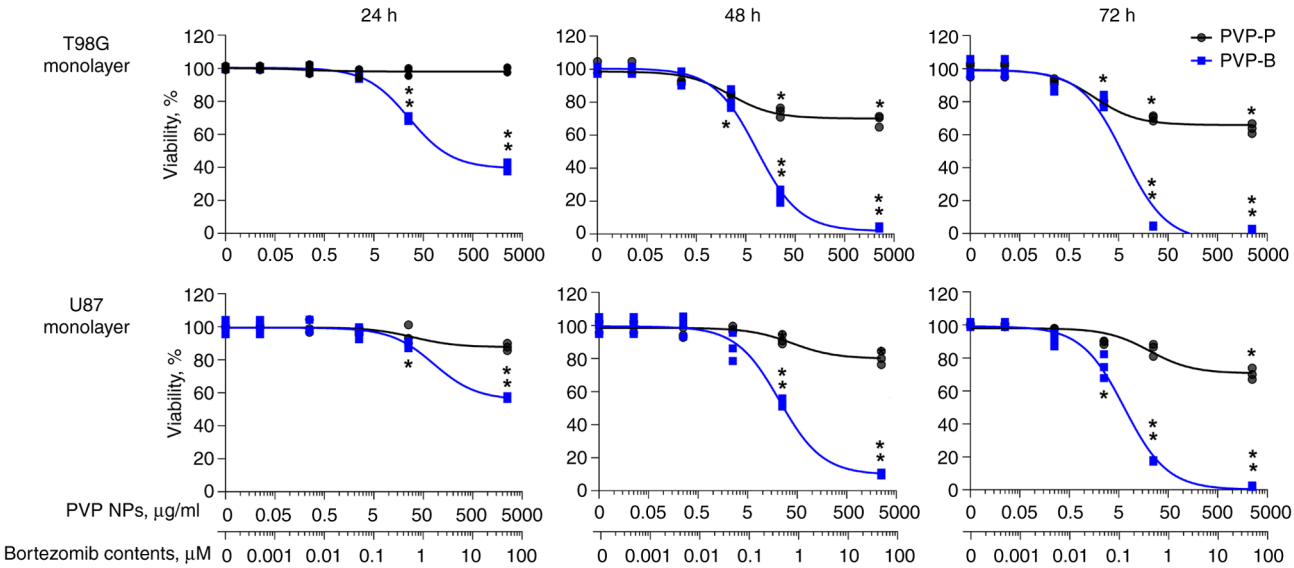

Figure 2. Cytotoxicity of amphiphilic PVP micellar NPs loaded with bortezomib (PVP-B) or prothionamide (PVP-P) in monolayer T98G and U87 human glioblastoma cell lines evaluated by MTT test after 24, 48 or 72 h of incubation. *P<0.05 and **P<0.01 by Student's t-test. PVP, poly(N-vinylpyrrolidone); NPs, nanoparticles.

bortezomib and prothionamide) was examined. The cytotoxicity of bortezomib-loaded PVP-B was lower than that of free bortezomib (IC_{50}=20.3±1.3 nM) (Fig. S1), considering the time required to release the substance from the hydrophobic core of the micelles. In support of the current results, neither hollow PVP polymer (Fig. S2), nor free prothionamide (Fig. S3) demonstrated signs of cytotoxic activity.

After 72-h incubation, PVP-B almost totally inhibited the viability of 3D tumor spheroids generated from human glioblastoma cells T98G (IC_{50}=8.5±2.7 μg/ml PVP-B, amounting to 272.0±8.6 nM of bortezomib contents) and U87 cells (IC_{50}=8.7±0.9 μg/ml PVP-B, 278.4±2.9 nM bortezomib) (Fig. 3). The morphology of spheroids demonstrated significant fragmentation, indicating cell death after incubation with PVP-B, but not with PVP-P (Fig. 4).

Additionally, the cytotoxicity of PVP-P and PVP-B was evaluated in normal cells. After 72-h incubation, neither of them revealed significant cytotoxicity in monolayer culture of normal human dermal fibroblasts (Fig. 5).

Evaluation of PVP-B toxicity in vivo in zebrafish. The *in vivo* toxicity of the bortezomib-loaded PVP-B nanoparticles was tested in zebrafish Danio rerio. Signs of acute toxicity were noted upon adding PVP-B to final concentration of PVP-B 30 mg/ml, manifested in increased motor activity of the tail and embryo death within the first h. When PVP-B was added at concentrations of 10 mg/ml, an increase in tail motor activity was observed, indicating the irritant toxic effect. A delay in tail development and spinal deformations were noted at PVP-B concentration of 3 mg/ml after 24-h incubation (Fig. 6). Death of 100% embryos was noted after 72-h incubation with 30, 10 and 3 mg/ml PVP-B, whereas at 0.3 mg/ml PVP-B, 83.3% of embryos succumbed. After 72-h incubation with 0.3 mg/ml PVP-B, developmental delays were observed in the surviving embryos. At concentrations 0.3, 3 and 10 mg/ml, PVP-B caused an enlargement of the yolk sac (Fig. 6). At 0.03 mg/ml PVP-B, no visible signs of toxicity were noted; 5 out of 6 (83.3%) embryos were alive both after 24 and 72-h incubation.

Therefore, the PVP-B toxicity was concentration-dependent, with mortality rising as the concentration increased. The LC_{50} was 0.1±0.011 mg/ml, as determined by regression analysis (Fig. 7), which is an order of magnitude higher compared with the cytotoxic doses in cancer cells.

Discussion

It is of great necessity for anticancer therapy to both expand the range of active substances delivered to tumors by nanoparticles, and broaden the range of cancer types that can be treated with nanosized antitumor drugs (20-23). Due to

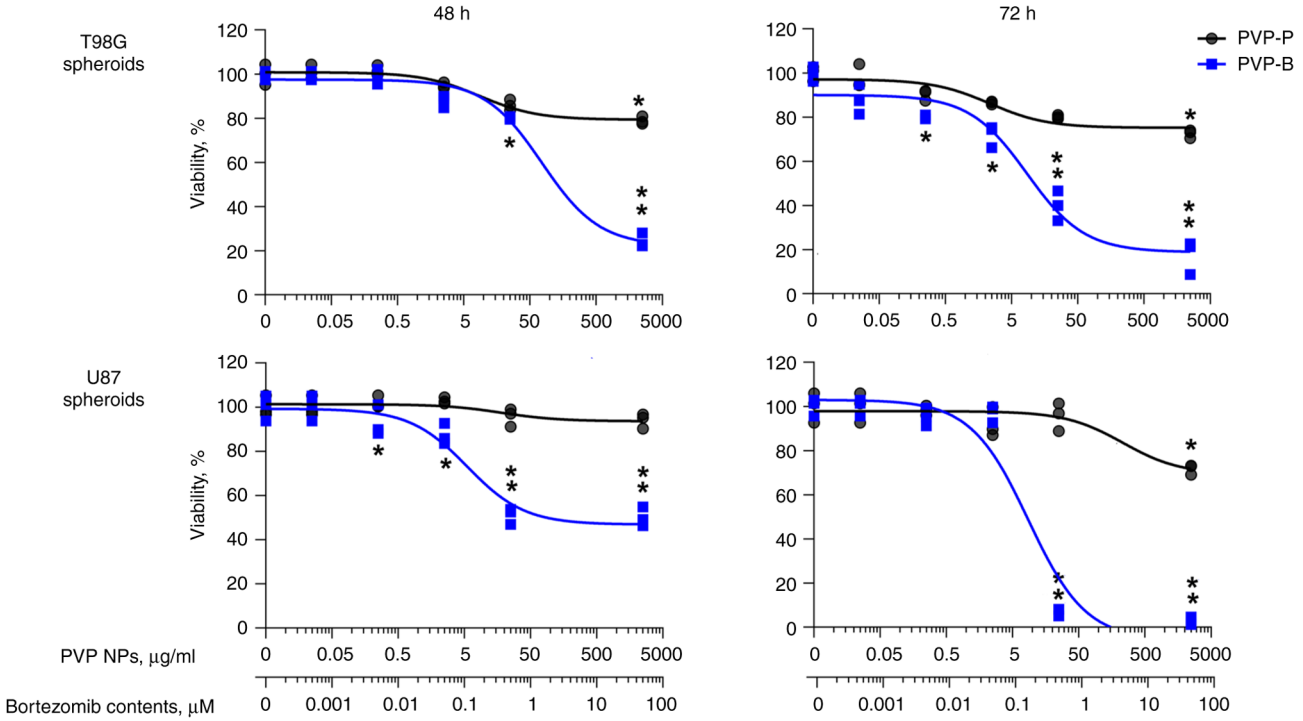

Figure 3. Cytotoxicity of amphiphilic PVP micellar NPs loaded with bortezomib (PVP-B) or prothionamide (PVP-P) in multicellular spheroids of human glioblastoma cells T98G or U87 evaluated by MTT test after 48 or 72 h of incubation. *P<0.05 and **P<0.01 by Student's t-test. PVP, poly(N-vinylpyrrolidone); NPs, nanoparticles.

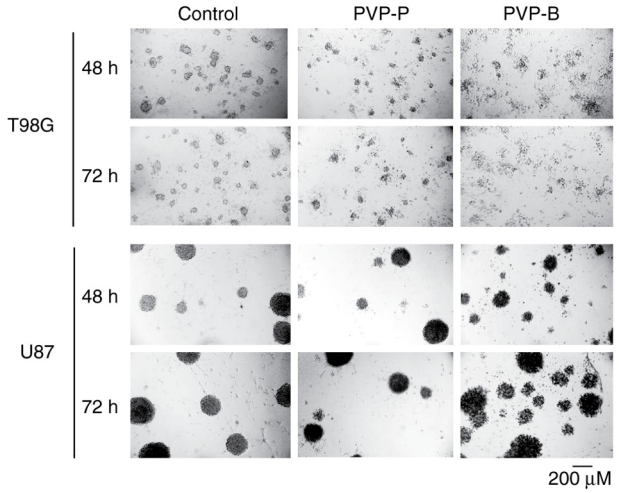

Figure 4. The morphology of 3D tumor spheroids generated from human glioblastoma cells T98G or U87 after incubation with 500 μg/ml of amphiphilic PVP micellar nanoparticles loaded with bortezomib (PVP-B) or prothionamide (PVP-P) for 48 h or 72 h. The spheroids were visualized using an inverted light microscope. Scale bar, 200 μm. PVP, poly(N-vinylpyrrolidone).

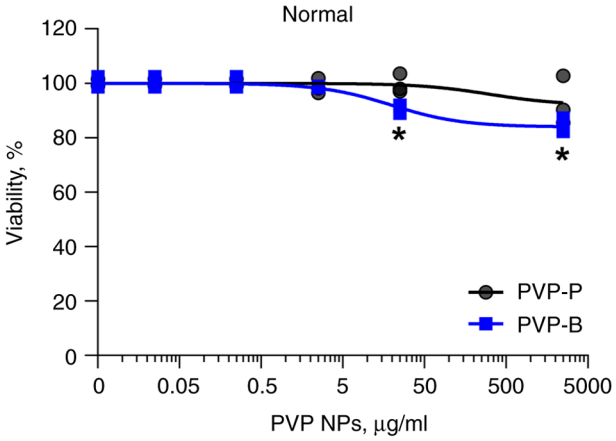

Figure 5. Cytotoxicity of amphiphilic PVP micellar NPs loaded with bortezomib (PVP-B) or prothionamide (PVP-P) in normal human fibroblasts after 72 h of incubation evaluated by MTT test. *P<0.05 by Student's t-test. PVP, poly(N-vinylpyrrolidone); NPs, nanoparticles.

poor pharmacokinetic properties, proteasome inhibition with bortezomib is approved only for the treatment of hematologic malignancies. However, if the poor serum stability and the side effects will be addressed, it may have therapeutic potential as part of a combinatorial strategy for the treatment of solid tumors, particularly brain cancer. A number of nanoscaled systems have been developed for delivery of bortezomib, such as liposomes, polymeric micelles, nanogels, dendrimers and biomimetic materials (7). For example, Gu *et al* (24) encapsulated bortezomib into hyaluronic acid-shelled and core-disulfide-crosslinked biodegradable micelles (HA-CCMs-BP) (24). Zhang *et al* (25) reported the co-delivery of bortezomib with paclitaxel in branched polyethyleneimine and palmitic acid nanoparticles. Unsoy *et al* (26) manufactured chitosan coated superparamagnetic iron oxide nanoparticles for magnetic targeting of bortezomib. De Santo *et al* (27) recently applied mesoporous silica-based nanodevice for bortezomib administration. Taking into account considerations of biocompatibility and safety of use, self-assembled polymer micelles have attracted remarkable attention due to their versatility, scalability

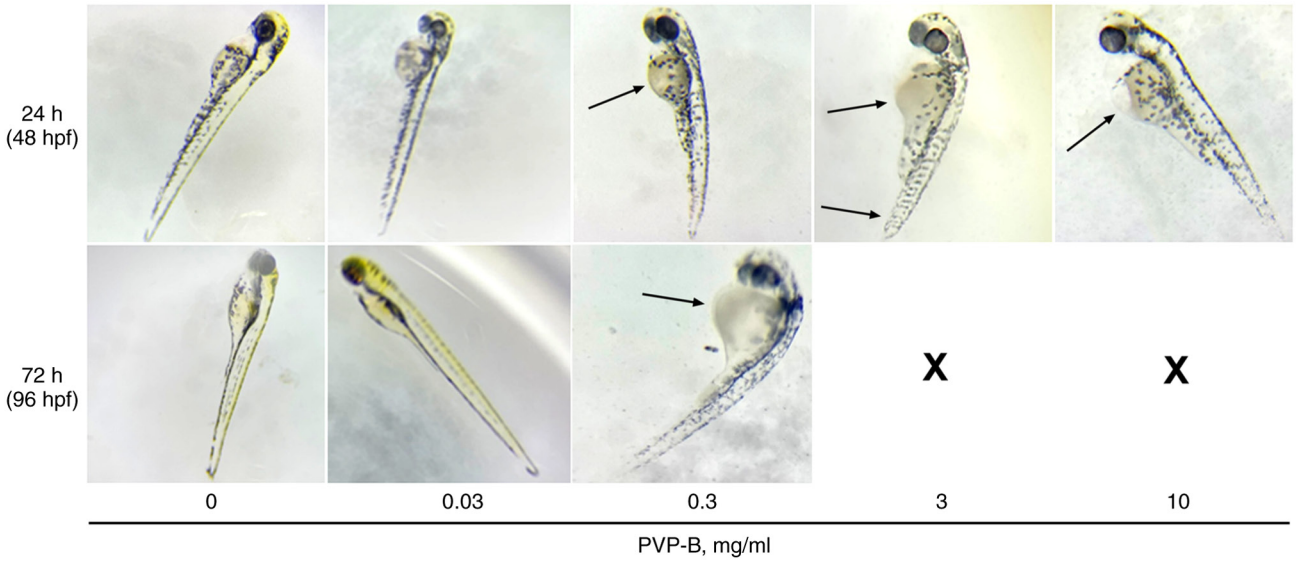

Figure 6. Zebrafish *Danio rerio* embryos after 24-h (48 hpf) and 72-h (96 hpf) incubation with bortezomib-loaded amphiphilic PVP micellar nanoparticles (PVP-B). Arrows indicate developmental delays. X indicates embryos' death. The images were captured using a Nexcope NSZ-810 microscope at x40 magnification. hpf, hours post-fertilization; PVP, poly(N-vinylpyrrolidone).

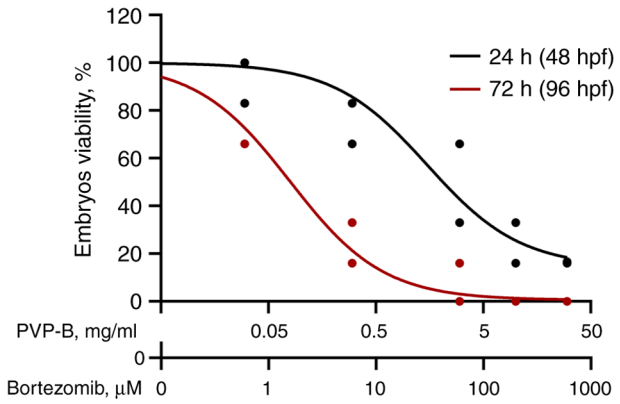

Figure 7. Survival of *Danio rerio* embryos (n=6 per group) during 24-h (48 hpf) and 72-h (96 hpf) incubation with bortezomib-loaded amphiphilic PVP micellar nanoparticles PVP-B. Lethal concentration 50% equals to 0.1 mg/ml of PVP-B and was determined by regression analysis using GraphPad Prism version 8.01. hpf, hours post-fertilization; PVP, poly(N-vinylpyrrolidone).

and suitability for wide range of applications (28). However, most of the previously reported polymeric micellar formulations bearing bortezomib contained polyethylene glycol (PEG) in their composition. For example, nanoparticles composed of amphiphilic copolymer PEG-block-poly(d,l-lactide) (29), PEG-poly(ε-caprolactone) (30), or pH-responsive diblock copolymers of PEG and catechol-functionalized polycarbonate with acid-labile acetal bond as a linker (31). Previously, there has been increasing concern about PEG regarding its tendency to activate complement (32) or accelerated blood clearance upon repeated injection (33).

PVP derivatives (Povidone K12, Kollidon®, Plasdone™,) are widely used in pharmaceuticals as excipients, blood substitutes, and inactive ingredients in intra-articular and intravenous drugs. In addition, povidone single-chain nanoparticles have been suggested as suitable for delivery of anticancer compounds cisplatin and lovastatin (34). In a previous study by the authors, the production of PVP micelles loaded with model substance prothionamide to stabilize the hydrophobic core was reported (14).

In the present study, antitumor drug bortezomib was loaded in the core of PVP micelles, aiming at reducing its toxicity and providing prolonged action. The specific activity was first assessed in the most common *in vitro* model of monolayer cell lines. The glioblastoma cells were chosen due to the prospects for the use of proteasome inhibitors against this aggressive brain tumor, provided that the problem of effective delivery of the drug to the lesion site is solved (35).

Importantly, it has been recently demonstrated by the authors that amphiphilic PVP nanoparticles loaded with lipophilic cargo are able to cross the blood-retina barrier (36). This suggests that a similar effect may be observed at the blood-brain barrier, justifying the selection of glioblastoma cell lines as a model object for cytotoxicity testing. In the present experiments, loading of bortezomib into micelles protected cells from immediate toxicity by prolonged drug release, since the cytotoxic activity of PVP-encapsulated bortezomib was time-delayed. Expectedly, 3D tumor spheroids were more resistant to PVP-B treatment compared with 2D monolayer tumor cell culture, indicating that they mimic solid tumors in an improved way compared with monolayer cells.

Additionally, the *in vivo* toxicity of the PVP-B nanoparticles was tested in zebrafish *Danio rerio* embyos. This model is distinguished by its accessibility and ability to quickly screen the toxicological and pharmacological effects of various substances, including nanoparticles, while reflecting *in vivo* metabolism issues in an improved way compared with *in vitro* models (37). Of note, the calculated LC_{50} of the PVP-B by an order of magnitude exceeded the IC_{50} in cancer cells *in vitro*, both 2D and 3D. This indicated that PVP-B micelles may have a therapeutic window between effective dose and dose-limiting toxicity. However, zebrafish model carry a set of limitations, such as methodology of drug dosing, translation of

administration, distribution, metabolism and excretion characteristics, and a set of specific biological characteristics which are different from mammals (38,39). Therefore, further *in vivo* experiments in mammals, including orthotopic intracranial xenograft model of human glioblastoma, will provide additional information regarding pharmacokinetic parameters, antitumor efficacy and safety. Additionally, since the ability of PVP-micelles to immobilize targeted protein has been previously demonstrated (14), this work may be continued in production of the micelles loaded with bortezomib and surface-modified with protein ligand for targeted drug delivery and a synergistic antitumor effect.

In conclusion, novel amphiphilic micellar PVP nanoparticles with encapsulated bortezomib may provide a safe and effective alternative to existing therapeutic regimens involving proteasome inhibitors due to high efficacy and possibly reduced side effects.

Acknowledgements

The TEM, DLS and zeta potential measurements were carried out using the equipment purchased on account of the Lomonosov MSU Development Program to 2020. The authors are grateful to Professor Sergey Burov (Cytomed JSC, St-Petersburg, Russia) for providing cyclic RGD-peptide.

Funding

The present study was supported by Russian Science Foundation (grant no. 23-15-00468; https://rscf.ru/project/23-15-00468/).

Availability of data and materials

All data generated or analyzed during this study are included in this published article.

Authors' contributions

ANK and AVY conceptualized the study. PPK, DVB, EVK and IIK curated data. ANK, DVB, AVY, MEG and IIK performed formal analysis. ANK, AVY, DAS and MEG acquired funding. PPK, DVB, PAP, EVK, AAI and IIK conducted investigation. ANK, DAS, AMT, MEG, DVB, AVY, EAM and VSP developed methodology. ANK and AVY performed project administration. ANK, DVB, MEG, EAM, AMT and VSP provided resources. ANK supervised the study. PPK, DVB, AVY, AEN, PCS, AMT and VSP validated data. DVB, EVK, IIK, AEN and AVY visualized data. AVY, DVB, IIK, AEN and PCS wrote the original draft. ANK, DVB, VSP, AMT, DAS and MEG wrote, reviewed and edited the manuscript. All authors read and approved the final version of the manuscript. ANK and AVY confirm the authenticity of all the raw data.

Ethics approval and consent to participate

Experiments performed on animals were carried out in accordance with the European Convention for the Protection of Vertebrate Animals Used for Experimental and Other Scientific Purposes. Experimental protocol was approved (approval no. 03p; May 16, 2023) by local ethics committee of the N.N. Blokhin National Medical Research Center of Oncology (Moscow, Russia).

Patient consent for publication

Not applicable.

Competing interests

The authors declare that they have no competing interests.

References

1. Zavrski I, Jakob C, Schmid P, Krebbel H, Kaiser M, Fleissner C, Rosche M, Possinger K and Sezer O: Proteasome: An emerging target for cancer therapy. Anticancer Drugs 16: 475-481, 2005.
2. Adams J and Kauffman M: Development of the proteasome inhibitor Velcade (Bortezomib). Cancer Invest 22: 304-311, 2004.
3. Raedler L: Velcade (Bortezomib) receives 2 new FDA indications: For retreatment of patients with multiple myeloma and for first-line treatment of patients with mantle-cell lymphoma. Am Health Drug Benefits 8: 135-140, 2015.
4. Cengiz Seval G and Beksac M: The safety of bortezomib for the treatment of multiple myeloma. Expert Opin Drug Saf 17: 953-962, 2018.
5. Yamamoto S and Egashira N: Pathological mechanisms of bortezomib-induced peripheral neuropathy. Int J Mol Sci 22: 888, 2021.
6. Tan CRC, Abdul-Majeed S, Cael B and Barta SK: Clinical pharmacokinetics and pharmacodynamics of bortezomib. Clin Pharmacokinet 58: 157-168, 2019.
7. Liu J, Zhao R, Jiang X, Li Z and Zhang B: Progress on the application of bortezomib and bortezomib-based nanoformulations. Biomolecules 12: 51, 2021.
8. Wen R, Umeano AC, Chen P and Farooqi AA: Polymer-based drug delivery systems for cancer. Crit Rev Ther Drug Carrier Syst 35: 521-553, 2018.
9. Waleka E, Stojek Z and Karbarz M: Activity of povidone in recent biomedical applications with emphasis on micro- and nano drug delivery systems. Pharmaceutics 13: 654, 2021.
10. Kuskov A, Nikitovic D, Berdiaki A, Shtilman M and Tsatsakis A: Amphiphilic poly-N-vinylpyrrolidone nanoparticles as carriers for nonsteroidal, anti-inflammatory drugs: Pharmacokinetic, anti-inflammatory, and ulcerogenic activity study. Pharmaceutics 14: 925, 2022.
11. Berdiaki A, Kuskov AN, Kulikov PP, Thrapsanioti LN, Giatagana EM, Stivaktakis P, Shtilman MI, Tsatsakis A and Nikitovic D: In vitro assessment of poly-N-Vinylpyrrolidone/acrylic acid nanoparticles biocompatibility in a microvascular endothelium model. Int J Mol Sci 23: 12446, 2022.
12. Villemson AL, Kuskov AN, Shtilman MI, Galebskaya LV, Ryumina EV and Larionova NI: Interaction of polymer aggregates based on stearoyl-poly-N-vinylpyrrolidone with blood components. Biochemistry (Mosc) 69: 621-628, 2004.
13. Berdiaki A, Perisynaki E, Stratidakis A, Kulikov PP, Kuskov AN, Stivaktakis P, Henrich-Noack P, Luss AL, Shtilman MM, Tzanakakis GN, *et al*: Assessment of amphiphilic poly-N-vinylpyrrolidone nanoparticles' biocompatibility with endothelial cells in vitro and delivery of an anti-inflammatory drug. Mol Pharm 17: 4212-4225, 2020.
14. Yagolovich A, Kuskov A, Kulikov P, Kurbanova L, Bagrov D, Artykov A, Gasparian M, Sizova S, Oleinikov V, Gileva A, *et al*: Amphiphilic poly(N-vinylpyrrolidone) nanoparticles conjugated with dr5-specific antitumor cytokine dr5-b for targeted delivery to cancer cells. Pharmaceutics 13: 1413, 2021.
15. Teng Y, Morrison ME, Munk P, Webber SE and Procházka K: Release kinetics studies of aromatic molecules into water from block polymer micelles. Macromolecules 31: 3578-3587, 1998.
16. Akasov R, Zaytseva-Zotova D, Burov S, Leko M, Dontenwill M, Chiper M, Vandamme T and Markvicheva E: Formation of multicellular tumor spheroids induced by cyclic RGD-peptides and use for anticancer drug testing in vitro. Int J Pharm 506: 148-157, 2016.
17. Kulikov PP, Kuskov AN, Goryachaya AV, Luss AN and Shtil'man MI: Amphiphilic poly-n-vinyl-2-pyrrolidone: Synthesis, properties, nanoparticles. Polym Sci Ser D 10: 263-268, 2017.

18. Kuskov AN, Kulikov PP, Luss AL, Goryachaya AV and Shtil'man MI: Preparation of polymer nanoparticles by self-assembling of amphiphilic poly-N-vinylpyrrolidone derivatives in aqueous media. Russ J Appl Chem 89: 1461-1468, 2016.
19. Kozulitsyna TI and Zemskova ZS: Therapeutic efficiency of ethionamide and prothionamide. Probl Tuberk 47: 66-69, 1969 (In Russian).
20. Radu IC, Hudita A, Zaharia C, Galateanu B, Iovu H, Tanasa EV, Georgiana Nitu S, Ginghina O, Negrei C, Tsatsakis A, *et al*: Poly(3-hydroxybutyrate-CO-3-hydroxyvalerate) PHBHV biocompatible nanocarriers for 5-FU delivery targeting colorectal cancer. Drug Deliv 26: 318-327, 2019.
21. Ginghină O, Hudiță A, Zaharia C, Tsatsakis A, Mezhuev Y, Costache M and Gălățeanu B: Current landscape in organic nanosized materials advances for improved management of colorectal cancer patients. Materials (Basel) 14: 2440, 2021.
22. Hudiță A, Radu IC, Zaharia C, Ion AC, Ginghină O, Gălățeanu B, Mărușescu L, Grama F, Tsatsakis A, Gurevich L and Costache M: Bio- and hemo-compatible silk fibroin PEGylated nanocarriers for 5-fluorouracil chemotherapy in colorectal cancer: In vitro studies. Pharmaceutics 13: 755, 2021.
23. Cicek B, Hacimuftuoglu A, Kuzucu M, Cetin A, Yeni Y, Genc S, Yildirim S, Bolat I, Kantarci M, Gul M, *et al*: Sorafenib alleviates inflammatory signaling of tumor microenvironment in precancerous lung injuries. Pharmaceuticals (Basel) 16: 221, 2023.
24. Gu Z, Wang X, Cheng R, Cheng L and Zhong Z: Hyaluronic acid shell and disulfide-crosslinked core micelles for in vivo targeted delivery of bortezomib for the treatment of multiple myeloma. Acta Biomater 80: 288-295, 2018.
25. Zhang R, Liu Y, Yang Z, Li Y, Rong X, Wang L, Guo C, Li S, Liu J, Li M and Wu Y: Construction of nanoparticles based on amphiphilic PEI-PA polymers for bortezomib and paclitaxel co-delivery. RSC Adv 5: 15453-15460, 2015.
26. Unsoy G, Yalcin S, Khodadust R, Mutlu P, Onguru O and Gunduz U: Chitosan magnetic nanoparticles for pH responsive Bortezomib release in cancer therapy. Biomed Pharmacother 68: 641-648, 2014.
27. De Santo M, Giovinazzo A, Fava M, Mazzotta E, De Napoli IE, Greco M, Comandé A, Nigro A, Argurio P, Perrotta I, *et al*: Engineered mesoporous silica-based nanoparticles as smart chemotherapy nanodevice for bortezomib administration†. Mater Chem Front 7: 216-229, 2023.
28. Yadav S, Sharma AK and Kumar P: Nanoscale self-assembly for therapeutic delivery. Front Bioeng Biotechnol 8: 127, 2020.
29. Shen S, Du XJ, Liu J, Sun R, Zhu YH and Wang J: Delivery of bortezomib with nanoparticles for basal-like triple-negative breast cancer therapy. J Control Release 208: 14-24, 2015.
30. Liu L, Wang S, Qi P, Song S, Yang Y, Shi J and Han G: Dopamine-modified poly(ε-caprolactone) micelles for pH controlled delivery of bortezomib. Int J Pharm 590: 119885, 2020.
31. Liu S, Ono RJ, Yang C, Gao S, Ming Tan JY, Hedrick JL and Yang YY: Dual pH-responsive shell-cleavable polycarbonate micellar nanoparticles for in vivo anticancer drug delivery. ACS Appl Mater Interfaces 10: 19355-19364, 2018.
32. Toda M, Arima Y and Iwata H: Complement activation on degraded polyethylene glycol-covered surface. Acta Biomate 6: 2642-2649, 2010.
33. Xu H, Ye F, Hu M, Yin P, Zhang W, Li Y, Yu X and Deng Y: Influence of phospholipid types and animal models on the accelerated blood clearance phenomenon of PEGylated liposomes upon repeated injection. Drug Deliv 22: 598-607, 2015.
34. Asenjo-Sanz I, Del-Corte M, Pinacho-Olaciregui J, González-Burgos M, González E, Verde-Sesto E, Arbe A, Colmenero J and Pomposo JA: Preparation and preliminary evaluation of povidone single-chain nanoparticles as potential drug delivery nanocarriers. Med One: 4: e190013, 2019.
35. Roth P, Mason WP, Richardson PG and Weller M: Proteasome inhibition for the treatment of glioblastoma. Expert Opin Investig Drugs 29: 1133-1141, 2020.
36. Tawfik M, Hadlak S, Götze C, Sokolov M, Kulikov P, Kuskov A, Shtilman M, Sabel BA and Henrich-Noack P: Live in-vivo neuroimaging reveals the transport of lipophilic cargo through the blood-retina barrier with modified amphiphilic poly-N-vinylpyrrolidone nanoparticles. J Biomed Nanotechnol 17: 846-858, 2021.
37. Pensado-López A, Fernández-Rey J, Reimunde P, Crecente-Campo J, Sánchez L and Torres Andón F: Zebrafish models for the safety and therapeutic testing of nanoparticles with a focus on macrophages. Nanomaterials (Basel) 11: 1784, 2021.
38. Gamble JT, Elson DJ, Greenwood JA, Tanguay RL and Kolluri SK: The zebrafish xenograft models for investigating cancer and cancer therapeutics. Biology (Basel) 10: 252, 2021.
39. Renieri EA, Sfakianakis DG, Alegakis AA, Safenkova IV, Buha A, Matović V, Tzardi M, Dzantiev BB, Divanach P, Kentouri M and Tsatsakis AM: Nonlinear responses to waterborne cadmium exposure in zebrafish. An in vivo study. Environ Res 157: 173-181, 2017.